machines

MDPI

Article

Research on Spraying Quality Prediction Algorithm for Automated Robot Spraying Based on KHPO-ELM Neural Network

Le Ling [1,†], Xuejian Zhang [2,3,†], Xiaobing Hu [2,3,*], Yucong Fu [2,3], Dongming Yang [2,3], Enpei Liang [1] and Yi Chen [1]

[1] Dongfang Electric Group Science and Technology Research Institute Company Limited, No. 18 Xixin Avenue, Gaoxin West District, Chengdu 611731, China; lingle@hotmail.com (L.L.); liangep0670@dongfang.com (E.L.); chenyi02@dongfang.com (Y.C.)
[2] School of Mechanical Engineering, Sichuan University, No. 24, South Section 1, First Ring Road, Chengdu 610065, China; advtechlab@stu.scu.edu.cn (X.Z.); fuyucong@stu.scu.edu.cn (Y.F.); 2021223025108@stu.scu.edu.cn (D.Y.)
[3] Institute of Industrial Technology, Sichuan University, Changjiang North Road, Yibin 644005, China
* Correspondence: huxb@scu.edu.cn
† These authors contributed equally to this work.

Abstract: In the intelligent transformation of spraying operations, the investigation into the robotic spraying process holds significant importance. The spraying process, however, falls within the realm of experience-driven technology, characterized by high complexity, diverse parameters, and coupling effects. Moreover, the quality of manual spraying processes relies entirely on manual experience. Thus, the crux of the intelligent transformation of spraying robots lies in establishing a mapping model between the spraying process and the resultant spraying quality. To address the challenge of intelligently transforming empirical spraying processes and achieving the mapping from the spraying process to spraying quality, an algorithm employing an enhanced extreme learning machine-based neural network is proposed for predicting spraying process parameters with respect to the evaluation index of spraying quality. In this approach, an algorithmic model based on the Extreme Learning Machine (ELM) neural network is initially constructed utilizing five spraying process parameters: spraying speed, spraying height, spraying width pressure, atomization pressure, and oil spraying pressure. Two spraying quality evaluation indexes, namely average film thickness at the center point and surface roughness, are also incorporated. Subsequently, the prediction neural network is optimized using the K-means improved predator optimization algorithm (KHPO) to enhance the model's prediction accuracy. This optimization step aims to improve the efficiency of the model in predicting spraying quality based on the specified process parameters. Finally, data collection and model validation for the spraying quality prediction algorithm are conducted using a designed robotic automated waterborne paint spraying experimental system. The experimental results demonstrate a significant reduction in the prediction error of the KHPO-ELM neural network model for the average film thickness center point, showcasing a decrease of 61.95% in comparison to the traditional ELM neural network and 50.81% in comparison to the BP neural network. Likewise, the improved neural network model yields a 2.31% decrease in surface roughness prediction error compared to the traditional ELM neural network and a substantial 54.0% reduction compared to the BP neural network. Consequently, the KHPO-ELM neural network, incorporating the prediction algorithm, effectively facilitates the prediction of multi-spraying process parameters for the center point of average film thickness and surface roughness in automated robot spraying. Notably, the prediction algorithm exhibits a commendable level of accuracy in these predictions.

Keywords: robotic spraying process; spraying process parameters; spraying quality evaluation index; KHPO; ELM

Citation: Ling, L.; Zhang, X.; Hu, X.; Fu, Y.; Yang, D.; Liang, E.; Chen, Y. Research on Spraying Quality Prediction Algorithm for Automated Robot Spraying Based on KHPO-ELM Neural Network. *Machines* **2024**, *12*, 100. https://doi.org/10.3390/machines12020100

Academic Editors: Marek Kočiško and Martin Pollák

Received: 28 December 2023
Revised: 22 January 2024
Accepted: 23 January 2024
Published: 1 February 2024

1. Introduction

Spraying is a method of dispersing paint into uniform and fine droplets and applying it to the surface of an object by means of a spray gun, using air pressure, which serves to cover and protect [1]. Spraying is a very important process in the processing of many products. It can provide anti-corrosion protection, insulation protection, wear protection and other auxiliary protection measures for mechanical parts in order to improve operating efficiency and service life in various types of harsh working environments [2]. The spraying process is an experience-driven technology [3]; the operation needs to rely on the operator's production experience to adjust the spraying process parameters. Therefore, a vast majority of factories still use manual spraying methods, which not only leads to huge labor costs, but also to low efficiency and unstable quality. In addition, harsh working environments and toxic and harmful substances in paints pose an occupational health hazard to the operators [4].

To address the challenges of inefficiency, unstable quality, and health hazards associated with manual spraying, technological upgrading of the spraying process is imperative. The transformation involves elevating the manual spraying process to an automated spraying production line with robotic operation [5]. This advanced production line seamlessly integrates industrial robotics technology with emerging Internet technologies such as neural networks and fuzzy control. It facilitates the learning and reuse of empirical manual processes, retaining the guiding role of manual experience while capitalizing on the unparalleled advantages of manual work in terms of iteration and generalization [6]. In comparison to manual spraying, robotic spraying boasts superior advantages, including heightened productivity, reduced production costs, enhanced spraying quality and quantity, optimal utilization of paint, and minimized health risks.

Despite these advantages, the design of the robotic spraying process is highly intricate owing to the numerous spraying process parameters involved and their strong coupling relationships [7]. For spraying robots, the core technical indicator is the quality of spraying. Balancing improved productivity with the achievement of high-quality spraying operations is crucial in the realm of robot spraying. Key evaluation indices for spraying quality primarily encompass the paint layer thickness and surface roughness of the sprayed components [8]. The current focal point of research in the robotic spraying process direction lies in establishing the role of the spraying parameter model and integrating spraying process modeling with spraying trajectory planning. Wu, HJ et al. introduced a method capable of predicting spraying thickness on complex part surfaces affected by shadowing effects. The method involves establishing a three-dimensional geometric model of the spraying contour based on Gaussian distribution, integrating robot trajectory and machining parameters. This approach not only creates a 3D geometric model of the spraying profile but also simulates spraying deposition in robot offline programming software. It concludes by visualizing the spraying morphology and predicted spraying thickness in a graphical virtual environment [9]. Zhang, YJ et al. proposed a predictive analytical model for the thickness of a spherical coated surface. Through numerical simulation and experimental testing, they demonstrated the model's effectiveness in predicting spraying thickness and uniformity with acceptable tolerance, particularly for spherical surfaces [10]. Gleeson, D et al. presented a paint spraying optimization method to refine the generated initial trajectory and minimize paint thickness deviation from the target thickness [11]. Gadow, R et al. introduced an advanced computer-aided robotic path planning method for thermal spraying. This method integrates optimization of generated trajectories and velocity profiles into coupled Computational Fluid Dynamics (CFD) and Finite Element Method (FEM) models, analyzing their effects on heat and mass transfer during spraying deposition [12]. Potkonjak, V et al. optimized the gun trajectory based on ergonomics and developed a spraying model for arbitrary gun position and attitude. The optimization resulted in reduced motor load, energy consumption, and need to control jitter [13]. Arikan, MAS et al. developed a methodology and computer program for modeling the painting process, simulating robotic painting, offline programming of industrial robots, and measur-

ing film thickness for curved surface painting. This comprehensive approach enables the simulation and analysis of spraying thickness [14].

While numerous relevant studies exist, several challenges persist. Firstly, the mathematical modeling of film thickness calculation exhibits a substantial gap between theoretical calculations and actual production and processing on-site, resulting in a lack of robustness in the film thickness calculation model. Secondly, the majority of studies on spraying distance, spray pressure, and other spraying parameters rely on qualitative research for simulation models. Due to the strong coupling effect among these parameters, the qualitative conclusions derived from such studies often diverge from actual processing, resulting in low feasibility in real-world applications. Consequently, utilizing field process parameter data and establishing a neural network-based prediction algorithm model incorporating multiple spraying process parameters emerges as the optimal solution to address the complexities of the field environment, offering high robustness, adaptability, and rapid iteration capabilities. This approach using neural networks for predicting and analyzing the quality of the spraying process presents advantages that the simulation model research method lacks [15].

Firstly, neural networks can model complex relationships owing to their substantial nonlinear fitting ability, allowing them to capture intricate relationships between input and output parameters. This capability enables the establishment of mapping relationships that explicit mathematical models cannot construct [16]. Secondly, neural networks exhibit strong generalization ability, providing reliable prediction results even in the face of unknown working conditions and parameter combinations by generalizing from training samples. Thirdly, neural networks allow flexible iteration, permitting the optimization of the combination of spraying process parameters through the correction of model training samples.

To address the aforementioned challenges, a prediction algorithm for spraying center film thickness and surface roughness based on multiple spraying process parameters and an improved Extreme Learning Machine neural network is proposed. This algorithm leverages neural networks, starting from the actual spraying processing site, to predict and evaluate the impact of spraying process parameters. The algorithm begins by studying the relationship between various spraying parameters and commonly used spraying quality evaluation indexes, selecting input and output parameters for the prediction model. Subsequently, the algorithm introduces the Extreme Learning Machine (ELM) neural network prediction algorithm model based on multiple spraying process parameters to map the spraying parameters to the spraying quality evaluation indexes. Finally, the prediction model for spraying quality evaluation indexes is optimized using the hyperparameter optimization (HPO) algorithm and the K-means clustering optimization algorithm. This optimization aims to enhance the convergence speed and global optimization ability of the prediction model. The proposed method enables the evaluation of spraying quality before robotic spraying operations, streamlining the optimization of the spraying process, reducing iterative costs associated with spraying operations, and ultimately enhancing the efficiency of process optimization.

2. Spraying Process

2.1. Spraying Process Parameters

This paper exemplifies the automated spraying of waterborne paints on flat parts to investigate the impact of spraying process parameters on spraying quality. Spraying quality is primarily influenced by spraying powder, the spraying process, and spraying equipment. Among these factors, the role of the spraying process is the most intricate and crucial [17]. In conjunction with the trajectory planning requirements of the spraying robot and the influence of process parameters, this paper consolidates the experimental scenarios established, focusing on the more pronounced effects of certain process parameters on spraying quality. These parameters include spraying speed, spraying height, spraying width pressure, atomization pressure, and oil spraying pressure.

Spraying speed refers to the velocity of paint particles ejected from the gun relative to the surface of the workpiece being processed. This parameter directly influences the thickness and uniformity of the paint layer. Excessive spraying speed leads to a too-thin layer of paint, which fails to adhere to the workpiece surface, while insufficient speed results in an overly thick layer, possibly leading to solidification or undesired flow.

Spraying height denotes the relative distance between the tip of the spray gun and the workpiece surface. Excessive or insufficient spraying height can cause an uneven paint layer. Spray width pressure refers to the gas pressure needed to create a fan-shaped pattern at the tip of the gun. This pressure significantly influences the distribution of spray particles and the stability of the spray pattern. Proper spray width pressure ensures uniformity in spraying. Atomizing pressure refers to the gas pressure at the tip of the gun responsible for atomizing paint into fine particles. This pressure greatly impacts the size and uniformity of sprayed particles. Adjusting atomizing pressure allows for further refinement of paint particles, contributing to a uniform coating. Oil spraying pressure represents the force propelling the liquid paint. The adjustment of oil spraying pressure affects the flow of paint and the size of the sprayed particles.

A robust observation reveals a pronounced coupling among the effects of spraying process parameters. The influence of a solitary parameter extends beyond its impact on coating quality, extending to the "gain" or "offset" of other parameters.

For instance, heightened spraying speeds may yield excessively thin coatings, whereas slower speeds may result in coatings of excessive thickness. Simultaneously, the spray height significantly influences coating thickness. Consequently, by concurrently adjusting spray speed and spray distance to strike a balance between speed and height, it becomes feasible to elevate the spray speed while concurrently achieving a coating thickness and uniformity aligning with process requirements. Furthermore, a coupling exists between spraying speed and spray width pressure. Elevated spraying speeds might necessitate higher spray width pressure, yet an excessively high pressure could yield particles of diminished size, adversely affecting coating uniformity. Hence, a careful equilibrium between spray speed and pressure is imperative to ensure that accelerated spray speeds do not compromise particle size, preserving coating uniformity. Additionally, a coupling relationship extends to spraying pressure parameters. Higher atomizing pressure may produce excessively small particles, while lower spraying pressure may result in uneven spray distribution. Consequently, consideration of spray pressure becomes integral when adjusting atomization pressure. Strategic adjustments guarantee a sufficiently high atomizing pressure, while maintaining the spray pressure within an optimal range to achieve uniform coating.

The intricate coupling among spraying parameters profoundly influences spraying quality. Consequently, in the analysis of spraying quality, it is imperative not only to scrutinize the impact of individual parameters but also to factor in the intricate interplay among multiple spraying process parameters.

2.2. Spraying Quality Evaluation Indexes

The quality evaluation of the paint film completed by the spraying robot involves the analysis and judgment of various characteristics, such as performance testing and characterization, to ensure compliance with processing requirements [18]. The inspection of coating quality primarily includes the detection of indicators like film thickness, adhesion, surface roughness, appearance, hardness, and corrosion resistance.

With consideration given to the designated experimental scenarios and the significance of quality indicators, the selection of evaluation indices in this paper focuses on the average film thickness and surface roughness at the center point. Due to the normal distribution of coating thickness in the robotic spraying process, the average film thickness at the center point is commonly utilized for evaluating the film thickness index. The center point's uniform film thickness, defined as the average of film thickness values measured at various

locations on the sprayed surface [19], directly signifies the uniformity of the paint film's surface area, a crucial aspect for coating quality.

Surface roughness, typically described in terms of surface parameters, characterizes the degree of microscopic unevenness on the surface of the object after spraying completion. The impact of surface roughness is direct on the adhesion, durability, and other properties of the paint layer.

Ensuring precision in high-precision mechanical products necessitates the meticulous control of the average film thickness and surface roughness at the coating center. This imperative is notably pertinent in the case of aero-engine blades and spacecraft housings, where the coating's height and surface roughness wield a considerable influence over aerodynamic performance, fuel efficiency, and structural durability during flight. By regulating the coating height and roughness, the hydrodynamic properties of the surface can be manipulated, thereby mitigating wind resistance and enhancing flight stability. Moreover, maintaining the coating within the ideal operational parameters effectively diminishes flight drag and surface friction, consequently augmenting fuel efficiency. In addition, adept control over coating height and roughness enables effective management of surface temperature and corrosion resistance. This adjustment, in turn, facilitates an extended service life and heightened reliability of the aircraft under challenging conditions, including high temperatures.

3. KHPO-ELM

3.1. ELM

The Extreme Learning Machine (ELM), introduced in 2006, is a type of single hidden layer feedforward neural network. It requires the initiation of hidden layer weights only once during training [20]. The ELM eliminates the need for backpropagation. Its accuracy depends on the number of models learned in training, resulting in quicker training speeds, simpler parameter adjustment, weight updates, and improved generalization ability.

The structure of the ELM network is depicted in Figure 1. In the training process of the ELM model, input layer weights and biases are randomly set, and output layer weights are calculated using generalized inverse matrix theory. Subsequently, data prediction is carried out by outputting information based on the obtained weights. The construction of the ELM neural network comprises four distinct stages.

1. According to the prediction objective, training sets X_i and t_i are set up with n samples.

$$X_i = [x_{i1}, x_{i2}, x_{i3}, \ldots, x_{in}]^T \in R^n, \tag{1}$$

$$t_i = [t_{i1}, t_{i2}, t_{i3}, \ldots, t_{im}]^T \in R^m, \tag{2}$$

   where x_i denotes the i_{th} data of the input matrix, and t_i denotes the labeling corresponding to the i_{th} data.
2. The hidden layer output o_j with L hidden layer nodes is computed.

$$o_j = \sum_{i}^{L} \beta_i g\left(W_i \cdot X_j + b_i\right), j = 1, 2, \ldots, N, \tag{3}$$

$$W_i = [w_{i,1}, w_{i,2}, w_{i,3}, \ldots, w_{i,n}]^T, \tag{4}$$

   where $g(x)$ is the activation function, W_i is the input weight, β_i is the output weight, b_i is the bias of the i_{th} hidden layer unit, and $W_i \cdot X_j$ is the inner product of W_i with X_j.
3. The output error is minimized by the existence of W_i, β_i, b_i, leading to the following Equation (5) holding true.

$$\sum_{j=1}^{N} \left\| o_j - t_j \right\| = 0, \tag{5}$$

$$t_j = \sum_{j=1}^{L} \beta_i g(W_i \cdot X_j + b_i), j = 1, 2, \ldots, N, \tag{6}$$

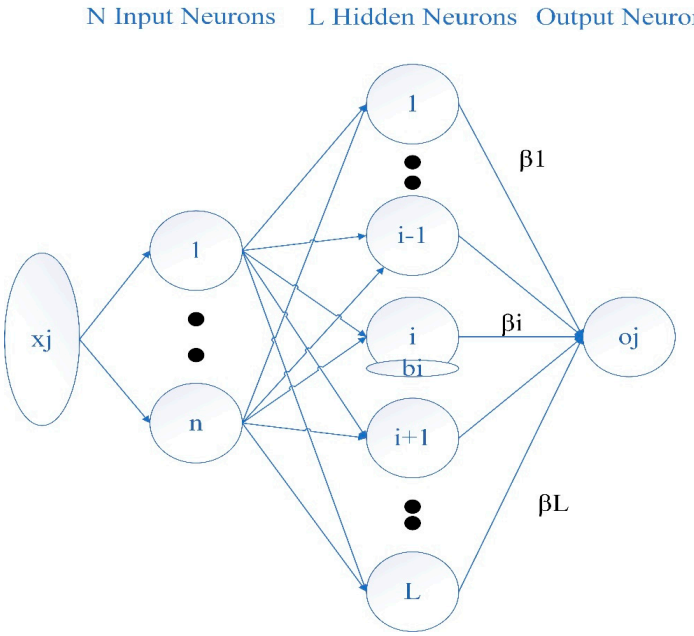

Figure 1. Structural diagram of the ELM neural network.

Leading to the matrix expression as:

$$H\beta = T, \tag{7}$$

$$H(W_1, W_2, \ldots, W_L, b_1, b_2, \ldots, b_L, X_1, X_2, \ldots, X_L) = \begin{bmatrix} g(W_1 \cdot X_1 + b_1) & g(W_L \cdot X_1 + b_L) \\ g(W_1 \cdot X_N + b_1) & g(W_L \cdot X_N + b_L) \end{bmatrix}_{N \times L} \tag{8}$$

$$\beta = \begin{bmatrix} \beta_1^T \\ \vdots \\ \beta_L^T \end{bmatrix}_{L \times m} \quad T = \begin{bmatrix} T_1^T \\ \vdots \\ T_N^T \end{bmatrix}_{N \times m}, \tag{9}$$

where H is the implicit layer node output, β is the output weight and T is the desired output.

The minimization loss function is E:

$$E = \sum_{j=1}^{N} \left(\sum_{j=1}^{L} \beta_i g(W_i \cdot X_j + b_i) - t_j \right)^2, \tag{10}$$

Through training, the optimal combination of $\hat{W}_i$, $\hat{\beta}_i$ and $\hat{b}_i$ parameters is obtained to maximize the model prediction accuracy.

3.2. KHPO

Due to the random generation of initialization weights and bias selection in the ELM neural network model, the accuracy is significantly impacted by different initial parameter settings. Additionally, the manual setting of hidden layer nodes in the model, along with the use of different node types, also plays a crucial role in performance. Consequently, employing optimization algorithms for global optimization and the automatic configuration of initial values and the number of hidden layer nodes in the ELM model holds significant importance in enhancing accuracy and convergence speed.

In this study, the ELM neural network model is optimized using a predator optimization algorithm. Proposed in 2022, the predator optimization algorithm achieves global optimization and rapid convergence by simulating the hunting process of animals [21]. The algorithm mimics the hunting process by continuously iterating the population search agent positions through the position update of the hunter and prey. It calculates the average position of the population, determines the distance between the search agent and the average agent using Euclidean distance, eliminates the maximum distance, and ultimately identifies the optimal position for optimization search.

The HPO algorithm flow is described below.

1. Initialization.

A random initialization community x_i is generated within the search range.

$$x_i = rand(1, d) * (ub - lb) + lb, \tag{11}$$

$$lb = [lb_1, lb_2, \cdots, lb_d], \tag{12}$$

$$ub = [ub_1, ub_2, \cdots, ub_d], \tag{13}$$

where x_i is the location of the search agent, lb is the lower bound of the variable, ub is the upper bound of the variable.

2. Hunter Location Updates;

$$x_{i,j}(t+1) = x_{i.j}(t) + 0.5\Big[\Big(2CZP_{pos(j)} - x_{i.j}(t)\Big) + \big(2(1-C)Z\mu(j) - x_{i.j}(t)\big)\Big] \tag{14}$$

$$P = \vec{R_1} < C, \tag{15}$$

$$IDX = (P == 0), \tag{16}$$

$$Z = R_2 \otimes IDX + \vec{R_3} \otimes (\sim IDX), \tag{17}$$

$$C = 1 - it\left(\frac{0.98}{MaxIt}\right), \tag{18}$$

where $x_{i.j}(t)$ is the current position of the hunter, $x_{i,j}(t+1)$ is the position of the hunter in the next cycle, C is the balance parameter, $P_{pos(j)}$ is the position of the prey, μ is the average value of the position, i denotes the number of cycles, j denotes the number of iterations, $\vec{R_1}$ and $\vec{R_3}$ are the random vectors in [0, 1], P is the index value of $\vec{R_1} < C$, R_2 is the random value in [0, 1], IDX is the index value when the constant P is equal to 0, it is the number of current iterations, and $MaxIt$ is the maximum number of iterations.

3. Prey location update;

Prey position p_{pos} is calculated:

$$\vec{p_{pos}} = \vec{x_i} \in sortedD_{euc}(kbest)p_{pos}, \tag{19}$$

$$\mu = \frac{1}{n}\sum_{i=1}^{n}\vec{x_i}, \tag{20}$$

$$D_{euc(i)} = \left(\sum_{j=1}^{d}\left(x_{i.j} - \mu_j\right)^2\right)^{\frac{1}{2}}, \tag{21}$$

$$kbest = round(C \times N), \tag{22}$$

where $\vec{p_{pos}}$ denotes the search agent with the largest distance from the mean. N is the number of search agents. After the location of the prey is determined, it is captured by the hunter through the decreasing mechanism $kbest$.

The prey location update formula is:

$$x_{i.j}(t+1) = T_{pos(j)} + CZ\cos(2\pi R_4) \times \left(T_{pos(j)} - x_{i,j}(t)\right) \tag{23}$$

where $x_{i,j}(t)$ is the current position of the prey, $x_{i.j}(t+1)$ is the position of the next iteration of the prey, $T_{pos(j)}$ is the global optimal position, and R_4 is a random number within $[-1, 1]$.

In the HPO optimization algorithm, when the initial search range is extensive, there is a noticeable reduction in both convergence speed and optimization finding ability. Therefore, this paper adopts the K-means algorithm for a secondary optimization of the initialization process in the HPO algorithm. The K-means algorithm is employed to partition the search space into different clusters, enhancing search efficiency and diminishing the time required for convergence [22].

Using the K-means algorithm, the samples within the initial interval of values for LEM parameters (HPO search space) are organized into k classes. The N data within the specified interval are distributed into k classes, ensuring that each sample has the minimum distance from the center of its respective class. This process can be considered as a potential grouping of hunters or prey during the initialization of the HPO, with each cluster having its own initial solution.

4. Method of Prediction

The evaluation index of spraying quality, the average film thickness, and surface roughness at the center point are subject to the combined effect of spraying speed, spraying distance, spraying width pressure, atomization pressure, and oil spraying pressure, which are expressed by the Equation (24):

$$\left(H_{avg}, R_a\right) \in D = \left\{D \middle| D(x) = f\left(V, D, P_{spray}, P_{atomization}, P_{oil}\right)\right\} \tag{24}$$

where H_{avg} represents the average film thickness at the center point; R_a represents the surface roughness; S is the distribution model obeyed by the quality parameters with regard to spraying; S has a close relationship with the spraying process parameters; V represents the spraying speed; S is the spraying distance; P_{spray} is the spraying width pressure; $P_{atomization}$ is the atomization pressure; P_{oil} is the oil spraying pressure. A detailed description of the symbols for each coating process parameter is provided in Appendix A.

Due to the existence of coupling between the spraying process parameters and the complexity of solving the explicit mathematical formulas, the mapping model of the spraying process parameters V, S, P_{spray}, $P_{atomization}$, P_{oil} to H_{avg} and R_a can be established by pre-experimental data samples of the multi-parameter role of the relationship between the data fitting and prediction of the results.

Founded on the advanced KHPO-ELM neural network framework, this paper introduces a predictive model employing a "5-input-2-output" neural network architecture tailored for forecasting multiple quality assessment metrics associated with diverse spraying parameters, as delineated in Figure 2. The model facilitates the prognosis of the average film thickness and surface roughness at the central point, predicated upon variables such as spraying speed, spraying distance, spraying width pressure, atomizing pressure, and spraying pressure.

Furthermore, with regard to the model, this study employs the HPO optimization algorithm to enhance the ELM neural network. Within this context, the global optimization capability and convergence speed of the ELM neural network are heightened through the optimization of input weights, output weights, and biases of hidden layer units. Additionally, the initialization process of the HPO algorithm undergoes quadratic optimization utilizing the K-means algorithm, thereby enhancing the search efficiency and iteration speed of the initial population in the HPO algorithm.

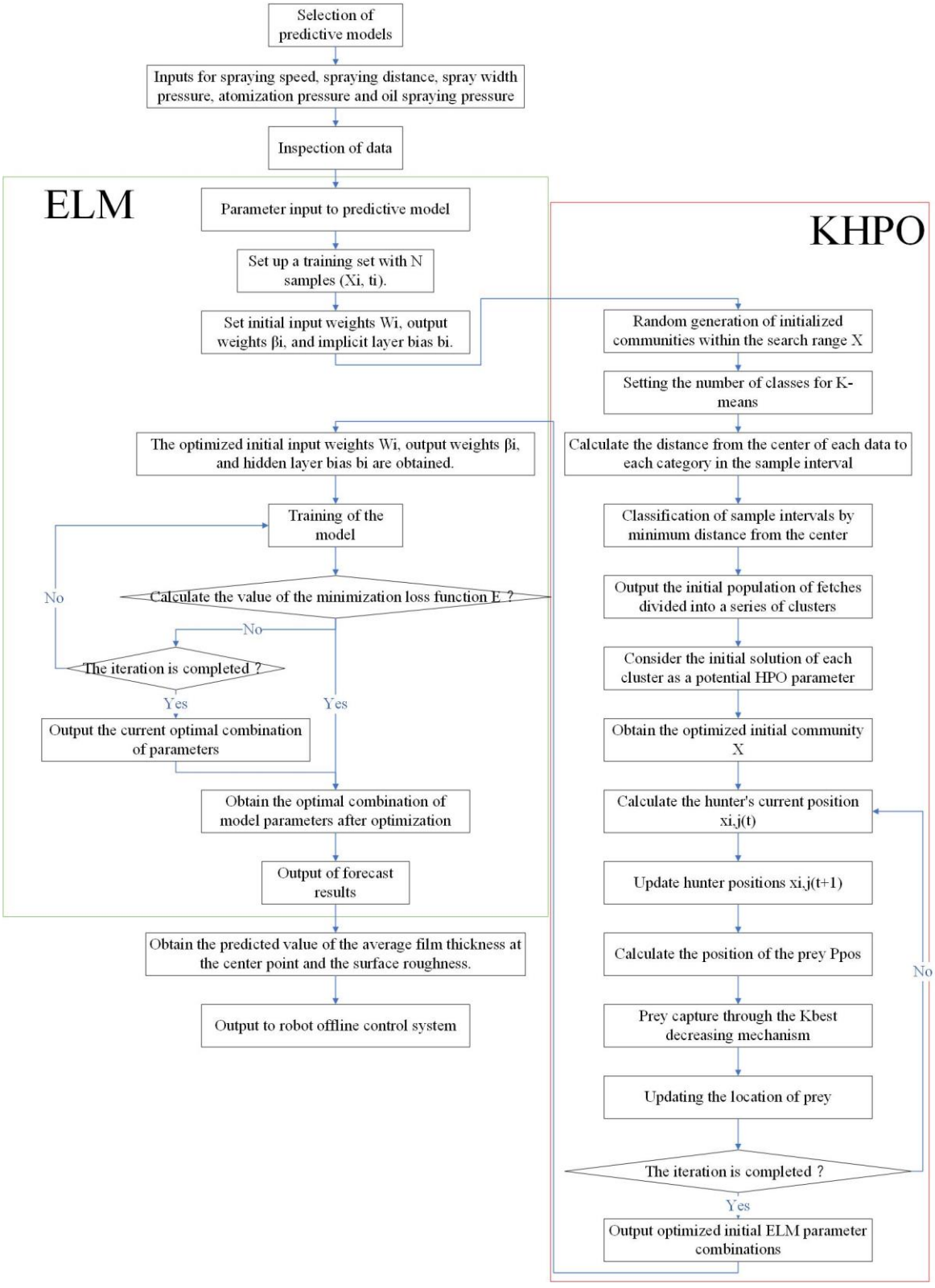

Figure 2. Block diagram of the process of spraying quality prediction algorithm based on multiple spraying parameters.

5. Experimental Methods

5.1. Experimental Settings

The experimental subject comprises ABB IR52 six-jointed robotic arm equipped with the GFA-200 automatic paint spray gun, utilizing the rock GFA-200 as the object of study. The research is conducted within an automatic offline spraying system, incorporating custom fixture devices, water-based paint, a magnetic thickness gauge, and a roughness detector. This configuration forms a robotic automated water-based paint spraying experimental system. The system serves as the foundation for designing pre-experiment data acquisition and validation experiments, ensuring the reliable verification of the spraying quality prediction model, as illustrated in Figure 3.

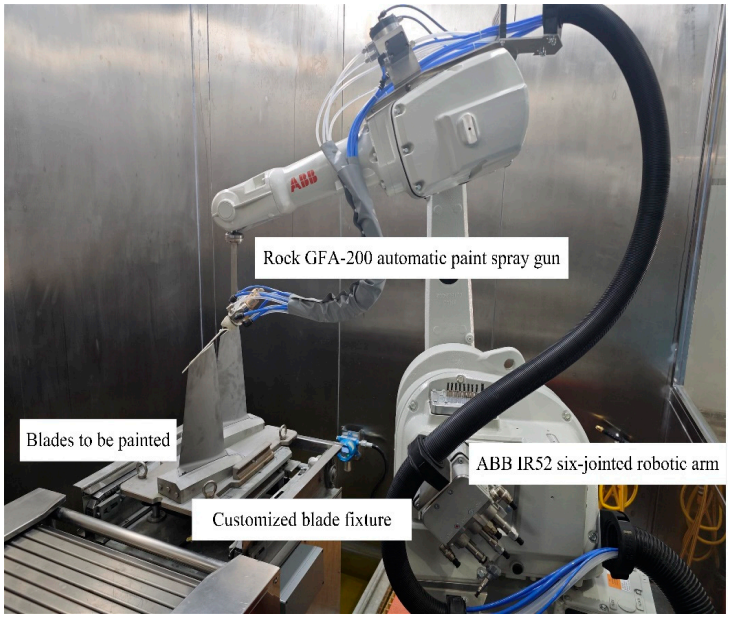

Figure 3. Automated Robotic Waterborne Paint Spraying Experiment System.

5.2. Acquisition of Data

To establish the mapping model capturing the coupling effect between spraying process parameters and spraying quality, this study devises flat waterborne paint spraying experiments involving five input parameters: spraying speed, spraying height, spraying width pressure, atomization pressure, and oil spraying pressure. These experiments, conducted with a magnetic thickness gauge and a roughness detector, evaluate the quality of sprayed plates based on the average film thickness at the center point and surface roughness. The obtained results reveal the impact of various spraying parameters on spraying quality.

The common value ranges for the five input parameters—spraying speed, spraying height, spray width pressure, atomization pressure, and oil spraying pressure—are presented in Table 1 below through the conducted study.

Table 1. Range of values for spraying process parameters.

Parameter	Value
Spraying speed	180 mm/min–280 mm/min
Spraying height	160 mm–230 mm
Spraying width pressure	0.10 MPa–0.17 MPa
Atomizing pressure	0.16 MPa–0.23 MPa
Oil spraying pressure	0.09 MPa–0.13 MPa

In orthogonal experiments, in order to target the study of the effect of the five input parameters, the robot end spraying angle is set at a constant 90° to exclude the interference of the spray gun factors, and at the same time, by ensuring the consistency of the experimental environmental conditions and the material conditions, to exclude the interference of factors such as temperature, humidity, plate, paint, and so on.

To systematically investigate the impact of the five input parameters, a five-factor, four-level orthogonal experiment is designed. The experimental parameter combinations are detailed in Table 2. Employing an isometric sampling approach, the five spraying input parameters are subjected to 3–5 sets of orthogonal experiments within the specified value interval. To mitigate the influence of random errors, three repetitive experiments are conducted to secure more accurate and comprehensive experimental samples and results.

Table 2. Parameter combinations of L16 (4&5) orthogonal experiments.

SN/Parameter	Factor 1: Spraying Speed (mm/min)	Factor 2: Spraying Height (mm)	Factor 3: Spraying Width Pressure (MPa)	Factor 4: Atomizing Pressure (MPa)	Factor 5: Oil Spraying Pressure (MPa)
1	1 (180–190)	1 (160–170)	1 (0.10–0.11)	1 (0.16–0.17)	1 (0.09–0.10)
2	1	2 (180–190)	2 (0.12–0.13)	2 (0.18–0.19)	2 (0.10–0.11)
3	1	3 (200–210)	3 (0.14–0.15)	3 (0.20–0.21)	3 (0.11–0.12)
4	1	4 (220–230)	4 (0.16–0.17)	4 (0.22–0.23)	4 (0.12–0.13)
5	2 (210–220)	1	2	3	4
6	2	2	1	4	3
7	2	3	4	1	2
8	2	4	3	2	1
9	3 (240–250)	1	3	4	2
10	3	2	4	3	1
11	3	3	1	2	4
12	3	4	2	1	3
13	4 (270–280)	1	4	2	3
14	4	2	3	1	4
15	4	3	2	4	1
16	4	4	1	3	2

Upon the completion of the spraying experiments, the collected experimental samples undergo center point average film thickness detection and roughness detection using a magnetic thickness gauge and a roughness detector. The magnetic thickness gauge employed in the spraying experiment is illustrated in Figure 4. Each sample undergoes three repetitive measurements, and the average of these measurements is considered the measured value for the average film thickness at the center point. The roughness tester utilized in the spraying experiment is depicted in Figure 5.

Figure 4. Magnetic Thickness Gauge.

5.3. Validation of Algorithms

In order to verify the reliability of the prediction model, 540 sets of experimental sample data are randomly disrupted in this paper to generate 540 sets of unordered

experimental datasets. Then the unordered datasets are divided into 530 sets of training data and 10 sets of testing data. The training datasets are used to construct the KHPO-ELM prediction model, and the test datasets are used to test the reliability of the model.

Figure 5. Roughness Detector.

In this paper, MATLAB software (v. R2022b) is used to build the KHPO-ELM prediction algorithm model for spraying quality of robotic spraying process with multiple inputs and multiple outputs. The initial parameters of the model are set using the experimental method; that is, model testing experiments are conducted for all possible parameters within a reasonable range of values. After several experiments, the model parameters summarized in this paper are shown in Table 3. The evolution curve of the model is depicted in Figure 6.

Table 3. Values of initial parameters of the KHPO-ELM prediction algorithm.

Parameter	Value
Number of neurons in the input layer of the ELM	5
Number of output layer neurons of ELM	2
Number of initial hidden layer neurons of ELM	50
Number of iterations of HPO	500
Population size of HPO	50
Upper and lower bound values of HPO	±1
Contraction factor of HPO	0.1
Initial value of K-means	30

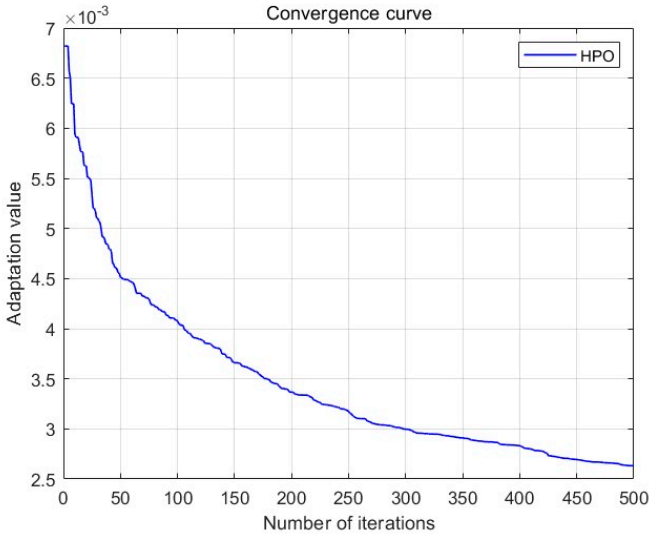

Figure 6. Evolutionary curve of the KHPO-ELM prediction algorithm.

6. Results

To demonstrate and validate the superior performance of the prediction network, two additional prediction models, BP and ELM, are established using the same set of data samples. All three models are input into the identical batch of the robotic automated waterborne paint spraying quality prediction system to assess the feasibility of these prediction models on the same group of test samples. The comparisons of MAE, MSE, RMSE, and MAPE for the prediction data obtained by the KHPO-ELM, ELM, and BP prediction networks are presented in Table 4. Further visual comparisons of predictions are depicted in Figure 7, prediction errors in Figure 8, and the mean absolute error of predictions in Figure 9.

Table 4. Comparison of errors of KHPO-ELM prediction model, ELM prediction model and BP prediction model.

Type	KHPO-ELM		ELM		BP	
	H_{avg}	R_a	H_{avg}	R_a	H_{avg}	R_a
MAE	0.8731	0.0719	2.2946	0.0736	1.7750	0.1563
MSE	0.9483	0.0068	7.6553	0.0077	5.2170	0.0289
RMSE	0.9738	0.0825	2.7668	0.0878	2.2841	0.1701
MAPE	1.4545	9.0026	4.0016	9.1725	2.9918	19.0310

Through validation experiments, the neural network prediction algorithm proves its capability to map coating process parameters to coating quality before the automated robotic coating operation. When compared with ELM and BP neural networks, the KHPO-ELM prediction network exhibits superior prediction accuracy for both the mean film thickness at the center point and surface roughness, eliminating the interference of error factors.

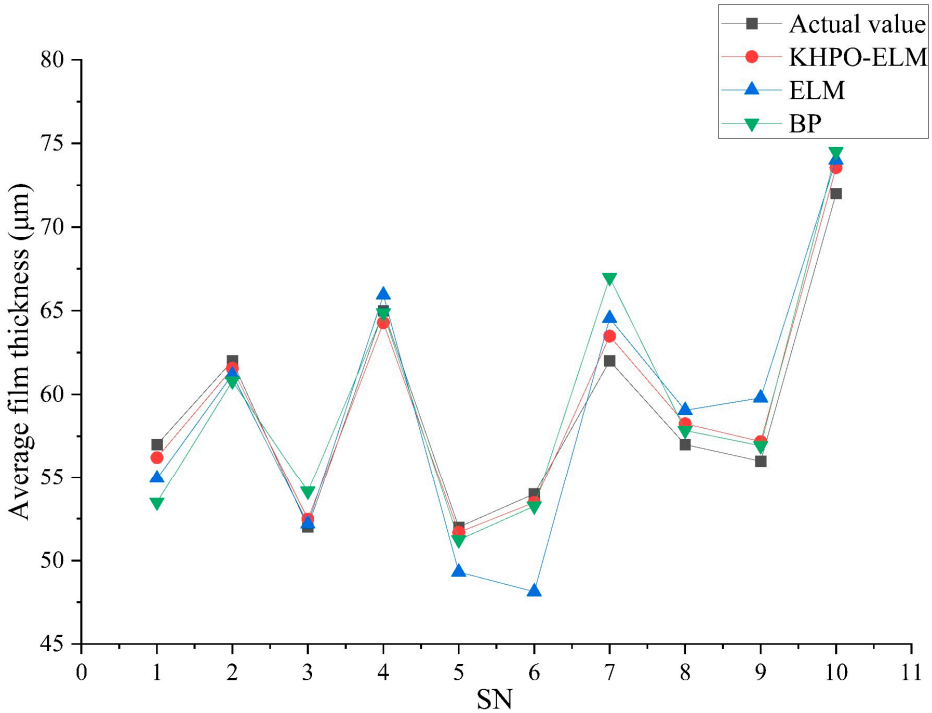

(**a**) H_{avg}

Figure 7. *Cont.*

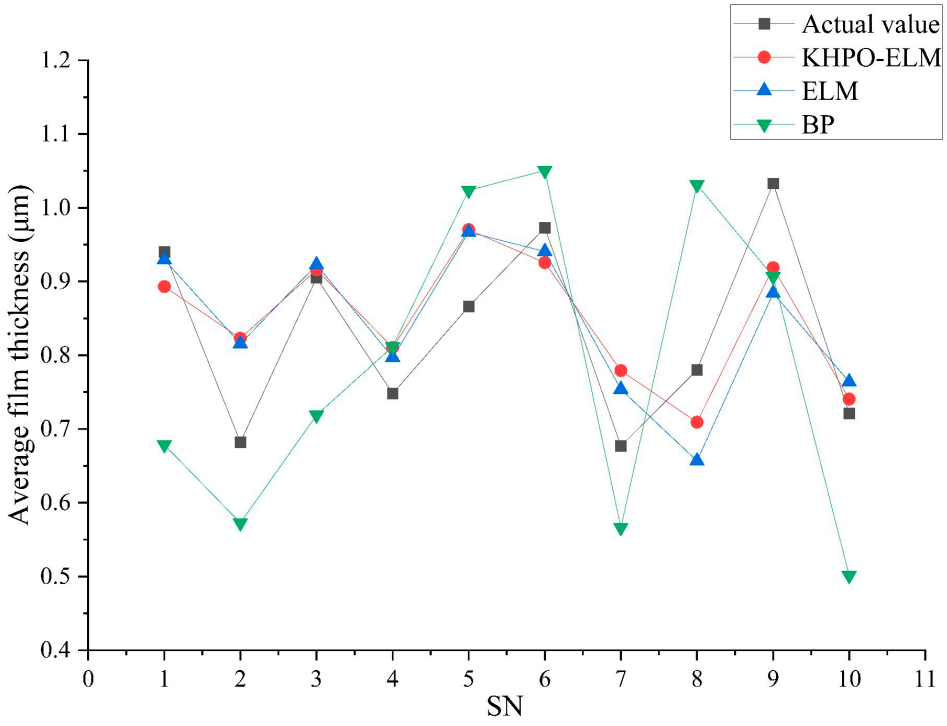

(**b**) R_a

Figure 7. Comparison of predicted values of KHPO-ELM prediction model, ELM prediction model, and BP prediction model.

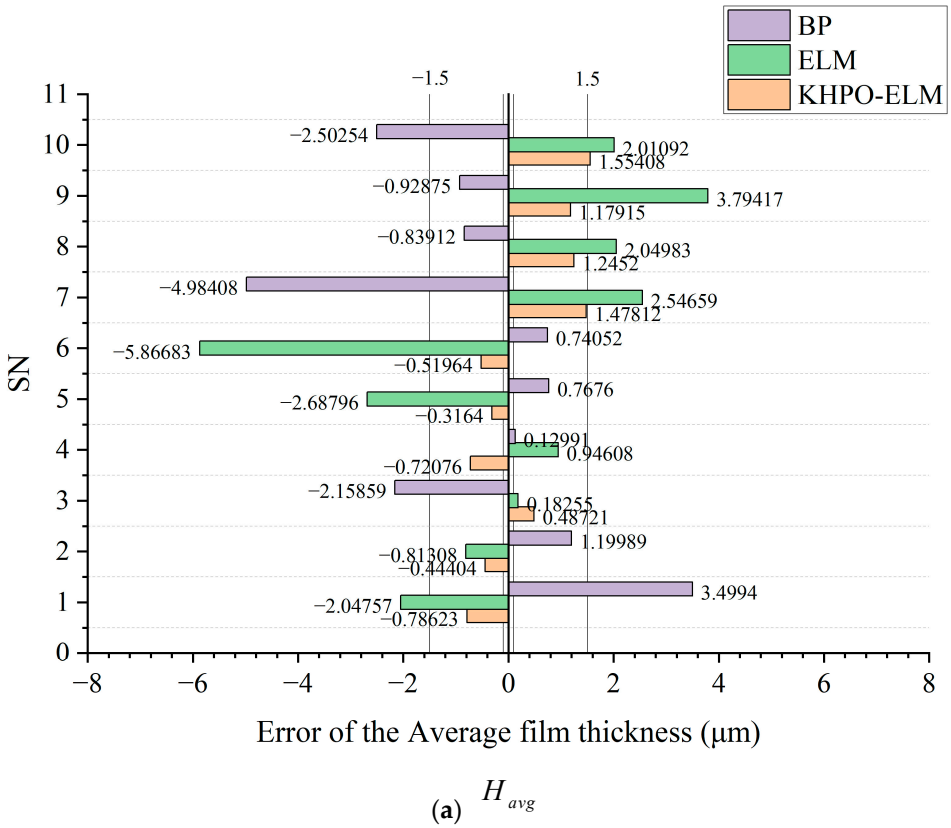

(**a**) H_{avg}

Figure 8. *Cont.*

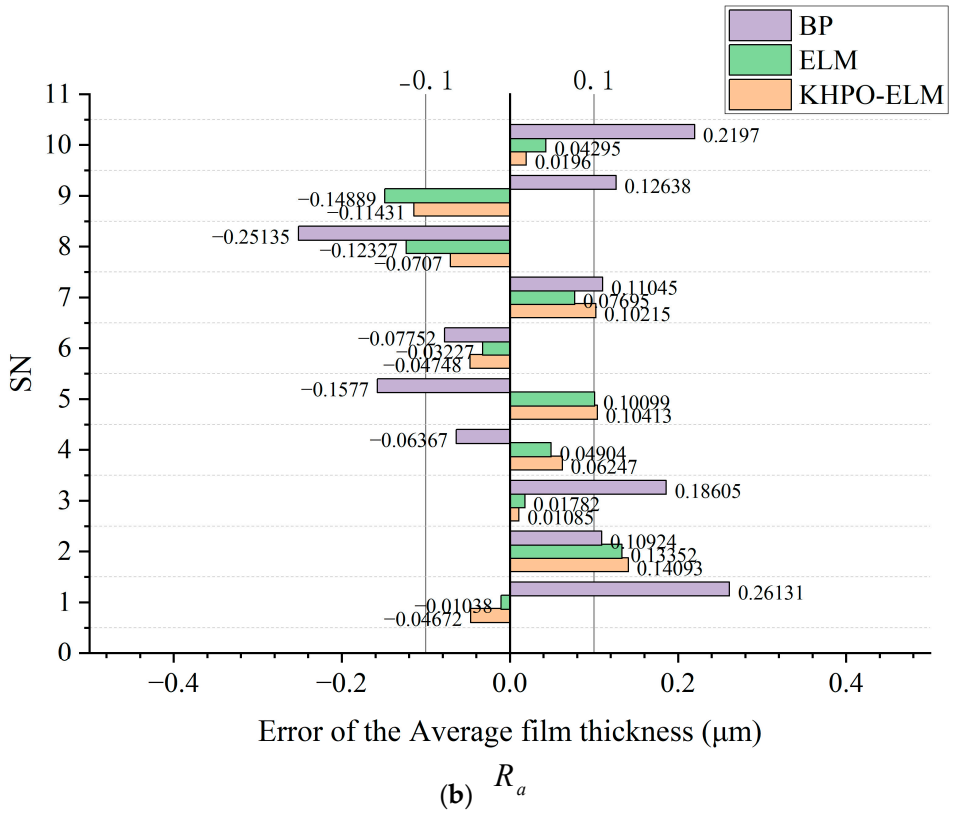

Figure 8. Comparison of errors of KHPO-ELM prediction model, ELM prediction model, and BP prediction model.

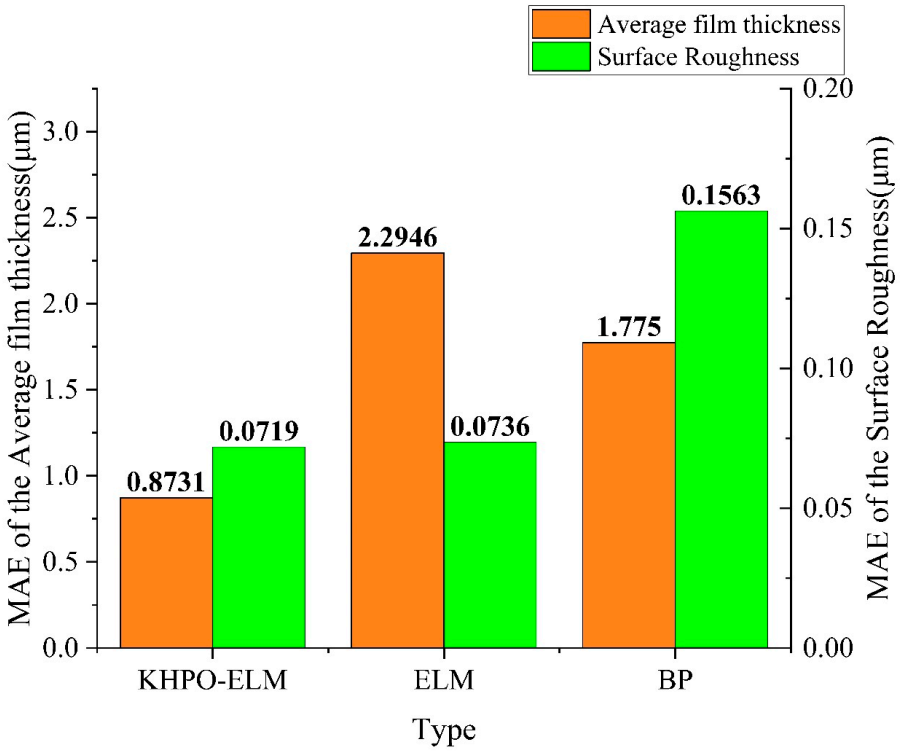

Figure 9. Evolutionary curve of the KHPO-ELM prediction algorithm.

The prediction model excels in forecasting the average film thickness at the center point of the paint film, with its MAE reduced to 0.8731 μm. The errors in the sample test results predominantly fall within ±1.5 μm, meeting the requirements of spraying operations. This reduction amounts to 61.95% and 50.81% when compared to the ELM and BP prediction models, respectively. Similarly, the KHPO-ELM prediction model performs admirably in predicting surface roughness, achieving an absolute average error reduced to 0.0707 μm. The sample test results mostly exhibit errors within ±0.1 μm, meeting the operational requirements. Compared to the ELM and BP prediction models, the error reductions are 2.31% and 54.00%, respectively.

7. Conclusions

(1) The robotic automated waterborne paint spraying process involves predicting the average film thickness at the center of the film and surface roughness, relying on five key spraying process parameters: spraying speed, spraying height, spray pressure, atomization pressure, and spray pressure. Despite the inherent variability in the spraying process, the accumulation of a substantial number of data samples allows for a detailed analysis and summarization of the impact of spraying process parameters during operations. Building upon this, a highly accurate, generalizable, and universal prediction algorithm is proposed, facilitating the rational prediction of spraying process parameters for quality spraying. This algorithm serves as a potent predictor for the application of spraying robots and the implementation of automated coating production lines, demonstrating wide applicability.

(2) In the prediction of coating quality in automated waterborne paint spraying processes by robots, the KHPO-ELM prediction algorithm model demonstrates superior prediction ability and lower prediction errors compared to the ELM and BP models. The MAE, MSE, RMSE, and MAPE indexes of the KHPO-ELM model outperform those of the other two models. The average error of the KHPO-ELM model is 61.95% and 50.81% lower than that of ELM and BP, respectively, ensuring all errors are controlled within approximately ±1.5 μm. Additionally, the average error of the absolute value of surface roughness prediction is 2.31% and 54.00% lower than that of ELM and BP, respectively, with all errors controlled within around ±0.1 μm. This aligns with the quality evaluation requirements of the spraying process.

(3) The core direction for the transformation and upgrading of the machinery industry, particularly in manufacturing processes heavily reliant on manual experience such as welding and grinding, is the substitution of people with robots. The nonlinear mapping model proposed in this paper, based on experimental data and neural networks, stands as a dependable solution to address challenges in this context. This intelligent prediction scheme holds promising applications in the industrial and intelligent transformation of the machinery industry. Primarily, the implementation of such a prediction scheme enhances the intelligence, flexibility, and efficiency of the production process. Additionally, in the realm of human-machine collaboration, this scheme supports machine learning to adapt to human operations and habits, thereby improving the collaborative efficiency between machines and humans. Furthermore, this solution is well suited for future implementation in decision support systems for intelligent mechanical operations. This system not only handles unexpected events adeptly but also optimizes the operational efficiency of mechanical systems. As for the intelligent prediction method, future developmental directions include enhancing the interpretability of the fitted model, improving data security and privacy protection, and advancing multimodal fusion. These aspects are anticipated to contribute to the ongoing evolution and refinement of this intelligent prediction approach.

Author Contributions: Conceptualization, L.L. and X.H.; methodology, X.Z.; software, X.Z.; validation, X.Z., Y.F. and D.Y.; formal analysis, X.Z.; investigation, E.L.; resources, Y.C.; data curation, Y.F.; writing—original draft preparation, L.L. and X.Z.; writing—review and editing, E.L. and X.H.; funding acquisition, Y.C. All authors have read and agreed to the published version of the manuscript.

Funding: This research was funded by the Sichuan University-Yibin School-City Strategic Cooperation Project, grant number 2020CDYB-3.

Data Availability Statement: Data are contained within the article.

Conflicts of Interest: Le Ling, Enpei Liang and Yi Chen are employees of the company.

Appendix A

Table A1. Description of notation.

Notation	Explanation	Unit
H_{avg}	The average film thickness at the center point	μm
R_a	The surface roughness	μm
D	The distribution model obeyed by the quality parameters with spraying	/
V	The spraying speed	mm/min
S	The spraying distance	mm
P_{spray}	The spraying width pressure	MPa
$P_{atomization}$	The atomization pressure	MPa
P_{oil}	The oil spraying pressure	MPa

References

1. Assadi, H.; Kreye, H.; Gärtner, F.; Klassen, T.J.A.M. Cold spraying–A materials perspective. *Acta Mater.* **2016**, *116*, 382–407. [CrossRef]
2. Sarikaya, O. Effect of some parameters on microstructure and hardness of alumina sprayings prepared by the air plasma spraying process. *Surf. Spray. Technol.* **2005**, *190*, 388–393. [CrossRef]
3. Almansoori, N.; Aldulaijan, S.; Althani, S.; Hassan, N.M.; Ndiaye, M.; Awad, M. Manual spray painting process optimization using Taguchi robust design. *Int. J. Qual. Reliab. Manag.* **2021**, *38*, 46–67. [CrossRef]
4. Park, R.M.; Bena, J.F.; Stayner, L.T.; Smith, R.J.; Gibb, H.J.; Lees, P.S. Hexavalent chromium and lung cancer in the chromate industry: A quantitative risk assessment. *Risk Anal. Int. J.* **2004**, *24*, 1099–1108. [CrossRef]
5. Arrais, R.; Costa, C.M.; Ribeiro, P.; Rocha, L.F.; Silva, M.; Veiga, G. On the development of a collaborative robotic system for industrial spraying cells. *Int. J. Adv. Manuf. Technol.* **2021**, *115*, 853–871. [CrossRef]
6. Evjemo, L.D.; Gjerstad, T.; Grøtli, E.I.; Sziebig, G. Trends in smart manufacturing: Role of humans and industrial robots in smart factories. *Curr. Robot. Rep.* **2020**, *1*, 35–41. [CrossRef]
7. Xie, F.; Liu, X.-J.; Wu, C.; Zhang, P. A novel spray painting robotic device for the spraying process in automotive industry. *Proc. Inst. Mech. Eng. Part C J. Mech. Eng. Sci.* **2015**, *229*, 2081–2093. [CrossRef]
8. Pendar, M.R.; Rodrigues, F.; Páscoa, J.C.; Lima, R. Review of spraying and curing processes: Evaluation in automotive industry. *Phys. Fluids* **2022**, *34*, 101301. [CrossRef]
9. Wu, H.; Xie, X.; Liu, M.; Chen, C.; Liao, H.; Zhang, Y.; Deng, S. A new approach to simulate spraying thickness in cold spray. *Surf. Spray. Technol.* **2020**, *382*, 125151.
10. Zhang, Y.; Li, W.; Zhang, C.; Liao, H.; Zhang, Y.; Deng, S. A spherical surface spraying thickness model for a robotized thermal spray system. *Robot. Comput.-Integr. Manuf.* **2019**, *59*, 297–304. [CrossRef]
11. Gleeson, D.; Jakobsson, S.; Salman, R.; Ekstedt, F.; Sandgren, N.; Edelvik, F.; Carlson, J.S.; Lennartson, B. Generating optimized trajectories for robotic spray painting. *IEEE Trans. Autom. Sci. Eng.* **2022**, *19*, 1380–1391. [CrossRef]
12. Gadow, R.; Candel, A.; Floristán, M. Optimized robot trajectory generation for thermal spraying operations and high quality sprayings on free-form surfaces. *Surf. Coat. Technol.* **2010**, *205*, 1074–1079. [CrossRef]
13. Potkonjak, V.; Đorđević, G.S.; Kostić, D.; Rašić, M. Dynamics of anthropomorphic painting robot: Quality analysis and cost reduction. *Robot. Auton. Syst.* **2000**, *32*, 17–38. [CrossRef]
14. Arikan, M.A.S.; Balkan, T. Process simulation and paint thickness measurement for robotic spray painting. *CIRP Ann.* **2001**, *50*, 291–294. [CrossRef]
15. Paturi, U.M.R.; Cheruku, S.; Geereddy, S.R. Process modeling and parameter optimization of surface sprayings using artificial neural networks (ANNs): State-of-the-art review. *Mater. Today Proc.* **2021**, *38*, 2764–2774. [CrossRef]
16. Cao, Y.; Zhao, J.; Qu, X.; Wang, X.; Liu, B. Prediction of Abrasive Belt Wear Based on BP Neural Network. *Machines* **2021**, *9*, 314. [CrossRef]
17. Yang, S.; Nie, W.; Lv, S.; Liu, Z.; Peng, H.; Ma, X.; Cai, P.; Xu, C. Effects of spraying pressure and installation angle of nozzles on atomization characteristics of external spraying system at a fully-mechanized mining face. *Powder Technol.* **2019**, *343*, 754–764. [CrossRef]
18. Wigren, J.; Täng, K. Quality considerations for the evaluation of thermal spray sprayings. *J. Therm. Spray Technol.* **2007**, *16*, 533–540. [CrossRef]

19. Pérez-Ramos, J.D.; Findlay, W.P.; Peck, G.; Morris, K.R. Quantitative analysis of film spraying in a pan coater based on in-line sensor measurements. *Aaps Pharmscitech* **2005**, *6*, E127–E136. [CrossRef]
20. Huang, G.B.; Zhu, Q.Y.; Siew, C.K. Extreme learning machine: Theory and applications. *Neurocomputing* **2006**, *70*, 489–501. [CrossRef]
21. Naruei, I.; Keynia, F.; Molahosseini, A.S. Hunter–prey optimization: Algorithm and applications. *Soft Comput.* **2022**, *26*, 1279–1314. [CrossRef]
22. Krishna, K.; Murty, M.N. Genetic K-means algorithm. *IEEE Trans. Syst. Man Cybern. Part B* **1999**, *29*, 433–439. [CrossRef]